Optics Communications 351 (2015) 45–49

Contents lists available at ScienceDirect

Optics Communications

journal homepage: www.elsevier.com/locate/optcom

Observing the transition from yoked superfluorescence to superradiance

Zhenhuan Yi [a,*], Pankaj K. Jha [a,b], Luqi Yuan [a], Dmitri V. Voronine [a,c], Gombojav O. Ariunbold [a,d], Alexander M. Sinyukov [a], Ziyun Di [a], Vladmir A. Sautenkov [a,e], Yuri V. Rostovtsev [f], Alexei V. Sokolov [a,c]

[a] Texas A&M University, College Station, TX 77843, USA
[b] Princeton University, Princeton, NJ 08544, USA
[c] Baylor University, Waco, TX 76798, USA
[d] National University of Mongolia, Ulaanbaatar 210646, Mongolia
[e] Joint Institute of High Temperature, RAS, Moscow 125412, Russia
[f] University of North Texas, Denton, TX 76203, USA

ARTICLE INFO

Article history:
Received 12 February 2015
Received in revised form
11 April 2015
Accepted 13 April 2015
Available online 15 April 2015

Keywords:
Yoked superfluorescence
Superradiance
Rubidium

ABSTRACT

We investigate cooperative emission from a rubidium vapor, and demonstrate a controlled transition from yoked superfluorescence to three-photon-induced superradiance by driving the medium with co-propagating ultrashort laser pulses. We study temporal emission profiles and time delays on a picosecond time scale and compare the measured pulse shapes with simulations. Our results suggest strategies to improve efficiency of mirrorless lasers and superradiant light sources.

1. Introduction

Superradiant light sources have recently been investigated as "sky lasers" for atmospheric remote sensing applications [1–4]. The efficiency of state-of-the-art backward lasers should be increased to enable many promising applications [5,6]. Laboratory-scale simple schemes can be used to mimic more complicated atmospheric experiments and to help understanding the basic physics. Furthermore, the possibility to generate superradiant UV and X-ray sources may lead to various biomedical applications [7,8].

In his seminal work, Dicke predicted enhancement of the spontaneous emission rate from a system of coherently excited atoms confined to a region with dimensions smaller than the wavelength [9]. This effect is known as Dicke superradiance (SR) [10,11]. Collective spontaneous emission from extended atomic samples was later studied by Eberly and Rehler [12]. The first experimental demonstration of the cooperative emission effect was performed by Skribanowitz et al. using optically pumped HF gas [13]. MacGillivray and Feld provided a theoretical explanation of how an initially inverted two-level system evolves into a superradiant state [14,15].

When the macroscopic dipole develops spontaneously in a system of incoherently excited atoms, the resulting cooperative emission is called superfluorescence (SF) [16,17]. SF also produces a short pulse similar to SR but with a characteristic time delay due to the time needed to generate the coherence. Recent experimental demonstrations of new SF sources were realized in atomic [18] and semiconductor systems [19]. In a three-level cascade scheme (Fig. 1), the radiation from the lower transition ($a \rightarrow b$) is generated by the coupling between the two-photon pumping ($b \rightarrow c$) and the SF between levels c and a. Thus the name yoked superfluorescence (YSF) is used to indicate the coupling of the two simultaneous radiation fields [20]. This phenomenon has been studied both theoretically [21,22] and experimentally [20,23–26]. Picosecond time-resolved studies of SR [27,28] and SF [29] were explored recently. Also the transitions between various regimes of cooperative emission based on the system parameters, such as the temperature or collisional dephasing, were investigated [30–32]. It is interesting to compare SR and YSF between the same atomic levels and to obtain laser control parameters to optimize intensity and pulse shape of the cooperative emission.

Here, we investigate the generation of the 420 nm radiation

* Corresponding author.
E-mail address: yzh@tamu.edu (Z. Yi).

http://dx.doi.org/10.1016/j.optcom.2015.04.035
0030-4018/

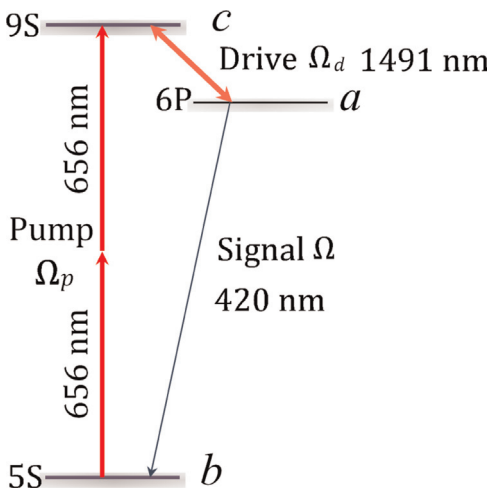

Fig. 1. Simplified energy level diagram of ^{87}Rb. Ω's are the Rabi frequencies of corresponding fields.

from an atomic vapor of ^{87}Rb. The atoms are excited by two photons from the 5*S* to 9*S* states by using ultrashort laser pulses centered at 656 nm (Fig. 1). We consider two scenarios. First, in the pure YSF, the pump pulse generates coherence between the 5*S* and 9*S* states and transfers population to the upper level, leading to population inversion and SF on the transition between the levels 9*S* and 6*P*. The coupling between the SF and the coherence generates 420 nm YSF radiation on the lower transition between 6*P* and 5*S* in the forward direction with respect to the pump pulse. The second scenario is a three-photon-induced SR process. We drive the 9*S* ↔ 6*P* transition by ultrashort laser pulses centered at 1491 nm and temporally overlapped with the pump pulse. We compare the 420 nm signals with and without the drive field. Numerical simulations using master equations are in a good qualitative agreement with the experimental results.

2. Experiment

The experimental setup is shown in Fig. 2. The 656 and 1491 nm, 60 fs laser pulses were collinearly focused into a thin 1.9 mm-long rubidium vapor cell. The cell is made of sapphire which allows high temperature operation and has a cylindrical shape with total length of 5.3 mm, two 1.7 mm-thick windows and a diameter of 1 in. The generated signal was analyzed using a spectrometer and a picosecond streak camera. The 656 nm (pump) and 1491 nm (drive) laser pulses were generated from two optical

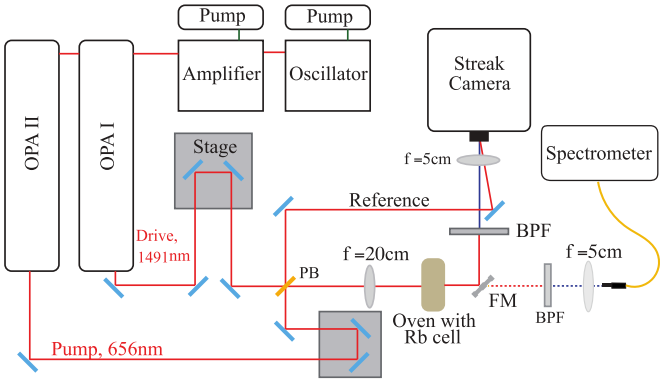

Fig. 2. Experimental setup for observing the transition from YSF to SR. The pump and drive laser pulses are collinearly combined and focused onto the Rb cell. FM is a flip mirror; BPF is a band-pass filter centered at 420 nm with FWHM of 10 nm.

parametric amplifiers (OPAs, Coherent) pumped by 800 nm, 30 fs laser pulses from a Ti:Sapphire femtosecond laser system (Coherent) with 1 kHz repetition rate. Both pulses were linearly polarized, with the same polarization. The pulse energy of each beam was controlled by a continuous variable neutral density filter. The drive beam was sent through a pair of 90-degree cornered mirrors mounted on a digitally controlled translation stage (Newport) to precisely adjust the time delay between the pump and drive pulses. Both beams were collinearly combined by a pellicle beamsplitter (PB) and were focused by a 200 mm focal length lens into the Rb cell. The number density of ^{87}Rb atoms was estimated to be 1.3×10^{15} cm^{-3}. The transmitted 656 nm beam after the PB was used as a reference for the streak camera. This beam and the generated signal from the cell were focused onto the entrance slit of the streak camera by a lens with focal length of 5 cm. The time resolution was optimized to ~2 ps.

3. Simulation

To get an insight into the temporal behavior of the SR signals in the experiment, a detailed numerical simulation was performed. The pump field (Ω_p) is two-photon resonant with the transition between the levels *b* and *c* (see Fig. 1). The drive field (Ω_d) is resonant with the upper transition between the levels *c* and *a*. The pump and drive fields are fully coherent laser pulses generated from OPAs as described in Section 2. They were modeled as Gaussian functions in Eqs. (2)–(6). The coherent drive field generates coherence between levels *c* and *a* which leads to cooperative emissions. The emitted field (Ω) is generated at the lower transition through the field propagation equation

$$\frac{\partial\Omega}{\partial z}+\frac{1}{c}\frac{\partial\Omega}{\partial t}=i\eta\rho_{ab}, \tag{1}$$

with the coupling constant $\eta=(3/8\pi)N\lambda^2\gamma$, where the atomic number density is $N\sim10^{15}$ cm^{-3}, the wavelength of this transition λ=420 nm, and the spontaneous emission rate $\gamma\sim6\,\mu s^{-1}$. The density matrix was calculated using the master equation [33]. The detailed simulation procedure can be found in reference [32]. Briefly we used the following equations:

$$\dot{\rho}_{ca}=-\Gamma_{ca}\rho_{ca}-i\Omega_d(\rho_{cc}-\rho_{aa})-i\Omega^*\rho_{cb}, \tag{2}$$

$$\dot{\rho}_{ab}=-\Gamma_{ab}\rho_{ab}-i\Omega(\rho_{aa}-\rho_{bb})+i\Omega_d^*\rho_{cb}, \tag{3}$$

$$\dot{\rho}_{cb}=-\Gamma_{cb}\rho_{cb}-i\frac{\Omega_p^2}{\Delta}(\rho_{cc}-\rho_{bb})+i\Omega_d\rho_{ab}-i\Omega\rho_{ca}, \tag{4}$$

$$\dot{\rho}_{cc}=-\gamma_{ca}\rho_{cc}+\left(i\Omega_d\rho_{ac}+i\frac{\Omega_p^2}{\Delta}\rho_{bc}+c.c.\right), \tag{5}$$

$$\dot{\rho}_{aa}=\gamma_{ca}\rho_{cc}-\gamma_{ab}\rho_{aa}+\left(-i\Omega_d\rho_{ac}+i\Omega\rho_{ba}+c.c.\right), \tag{6}$$

$$\rho_{aa}+\rho_{bb}+\rho_{cc}=1, \tag{7}$$

where Ω's are the Rabi frequencies of corresponding fields; ρ's are components of density matrix; Γ_{ij} is the decoherence rate between level *i* and level *j*, γ_{ij} is the spontaneous decay rate from level *i* to level *j*, and Δ is the single photon detuning between the pump field and the nearest intermediate state (which is state 5*P* in this case).

The pump and drive pulses were focused into a 1.9-mm-long pencil-like active medium with the cross-sectional area of 10^{-9} m^2. The pump field generates coherence ρ_{cb} and transfers part of the population into the level *c*. If there is no drive field,